Chemical Physics Letters 730 (2019) 497–505

Contents lists available at ScienceDirect

Chemical Physics Letters

journal homepage: www.elsevier.com/locate/cplett

Research paper

The ^2S Rydberg series of the lithium atom. Calculations with all-electron explicitly correlated Gaussian functions

Amir Bralin[a], Sergiy Bubin[a], Monika Stanke[b], Ludwik Adamowicz[c,d,*]

[a] Department of Physics, School of Science and Technology, Nazarbayev University, Astana 010000, Kazakhstan
[b] Institute of Physics, Faculty of Physics, Astronomy, and Informatics, Nicolaus Copernicus University, ul. Grudzia˛dzka 5, Toruń PL 87-100, Poland
[c] Department of Chemistry and Biochemistry and Department of Physics, University of Arizona, Tucson, AZ 85721, USA
[d] Interdisciplinary Center for Modern Technologies, Nicolaus Copernicus University, ul. Wileńska 4, Toruń PL 87-100, Poland

HIGHLIGHTS

- High-accuracy calculations for the 12 ^{2}S Rydberg states of Li.
- Finite-nuclear-mass approach is used.
- Isotope shifts of the transition energies are calculated.
- All-electron explicitly correlated Gaussian functions are used.
- The non-linear parameters of the Gaussians are optimized.
- Analytical energy gradient is used in the optimization.
- For the 10s, 11s, 12s, and 13s states the present calculations are the first ever.

ABSTRACT

In this work we report very accurate variational calculations of the twelve lowest ^2S Rydberg states of the lithium atom performed with the finite-nuclear-mass (FNM) approach and with all-electron explicitly correlated Gaussian functions. The FNM non-relativistic variational energies of the states are augmented with the leading relativistic and QED corrections. The calculated transition energies are compared with the previous works (only eight states of the series were calculated before) and with the available experimental results. Density distributions of the electrons and the nucleus in the center-of-mass frame are also shown.

1. Introduction

One of the major challenges of the quantum theory of atoms is to determine the energy levels corresponding to bound ground and excited states and the frequencies of the transitions between these levels with the spectroscopic accuracy (i.e. below 1 cm^{-1}). As such determination involves the calculation of the corresponding wave functions representing the computed states, various properties of the states can also be determined. That involves, for example, the transition intensities, the average distances of the electrons to the nucleus and between the electrons, etc. As the amount of computations required grows very rapidly with the number of electrons (this growth is proportional to the factorial of the number of electrons) even for atoms with a few electrons this becomes a computationally very demanding task. Thus, in undertaking such calculations the accuracy one aims to achieve needs to be balanced with the computational resources the calculations are expected to use.

One of the many challenges involved in atomic calculations is to target not only a few lowest lying states but to extend the calculations to a wider spectrum of states. For the lithium atom calculations exist where excited-state energies and the corresponding wave functions were determined with high accuracy using various approaches such as: multi-reference self-consistent-field, full configuration interaction, Hylleraas-configuration-interaction, etc. [1–8]. Particularly relevant to the present work are the most recent calculations performed by Drake and Yan, Wang et al., and Puchalski et al. [2,7,8]. For the beryllium atoms only the lowest five ^1S states [9] and one ^1P state [10] were calculated. Recently, very accurate calculations were also performed for the lowest four ^2S states of the boron atom [11]. Capabilities now exist to extend the calculations of Rydberg states of small atoms to ten states and beyond. In this work such calculations are reported for two isotopologues of the lithium atom (^{6}Li and ^{7}Li). The ^2S Rydberg series is

* Corresponding author.
E-mail addresses: amir.bralin@nu.edu.kz (A. Bralin), sergiy.bubin@nu.edu.kz (S. Bubin), monika@fizyka.umk.pl (M. Stanke), ludwik@email.arizona.edu (L. Adamowicz).

https://doi.org/10.1016/j.cplett.2019.06.051
Received 24 April 2019; Received in revised form 17 June 2019; Accepted 18 June 2019
Available online 19 June 2019

being considered.

Very accurate calculations of atomic spectra, especially when highly excited Rydberg states are being considered, is a challenging undertaking. Electron correlation, the effect originating from strong Coulombic interaction between the electrons, needs to be very accurately described. Moreover, there are some subtle effects due to relativism, QED, and finite nuclear mass and size that need to be also accounted for in the calculation. The most accurate description of the correlated motion of the electrons can be achieved if the basis functions used for expanding the spatial part of the wave function explicitly depends on the distances between the electrons (the so-called explicitly correlated basis functions). The explicitly correlated Gaussian functions (ECG) used in the present calculations are such functions. They were introduced to the field of atomic and molecular quantum-mechanical calculations by Boys [12]. An example of ECG atomic calculations is the work on the determination of the $3^1S \rightarrow 2^1S$ transition energy of the beryllium atom [13] where the calculated value agreed with the experimental results of Johansson [14,15] within the experimental error bar. ECGs were also used to calculate the lowest $S \rightarrow P$ transitions of beryllium [10].

The standard approach to calculate atomic spectra involves in the first step a calculation of the total non-relativistic energies of the considered states of the system with an infinite nuclear mass (INM). Subsequently, in the following steps the perturbation theory is used to account for energy corrections (adiabatic and non-adiabatic) due to the finite nuclear mass (FNM), as well as for relativistic and quantum-electrodynamics (QED) effects and effects due to the finite size of the nucleus. The leading corrections are calculated as expectation values of the corresponding quantum mechanical operators representing the effects. In the present work the non-relativistic calculations in the first step are performed using the FNM approach. Thus, the resulting energies and the corresponding wave functions depend on the nuclear mass of the considered isotopologue. Most of the adiabatic and non-adiabatic effects are already explicitly included at this stage of the calculation. In the approach used, the Hamiltonian representing the atom is first written in terms of Cartesian laboratory coordinates and then it is transformed to a new Cartesian coordinate system, whose first three coordinates are the laboratory-frame coordinates of the center of mass and the remaining coordinates are internal coordinates. In calculating the energy corrections due to relativistic and QED effects, the quantum mechanical operators representing these effects are also first transformed from the laboratory coordinate system to the new coordinate system and then they are used to calculate the corrections. As the leading corrections are expectation values of the operators calculated using the FNM wave functions, they are also specific to the particular istopologues. This means that the so-called recoil effects are explicitly included in the corrections and do not need to be calculated using an approach based on the double perturbation theory.

Various types of ECG basis functions have been used by our research group in high-accuracy accurate atomic and molecular calculations performed with an approach where the Born-Oppenheimer (BO) approximation has not been assumed and an approach based on the BO approximation [16,18,19]. High accuracy in those calculations have been achieved by performing extensive optimization of the non-linear parameters of the Gaussians by the variational minimization of the total energy of the system. To expedite the minimization, we have developed and implemented algorithms for calculating analytical derivatives of the total energy with respect to the non-linear parameters of the ECGs (i.e. the energy gradient) [16,17]. The implementation of the energy gradient, which is supplied to the optimization procedure to guide the process of changing the values of the non-linear parameters to lower the energy, has been key to generate very accurate results in the calculations. Thus, even though the Gaussians less accurately describe the cusps and the long-range behavior of the wave function in comparison with, for example, explicitly-correlated Slater functions, this deficiency can be effectively remediated with the use of sufficiently large ECG basis sets and by optimizing them with a gradient-based optimization procedure.

If a FNM approach is employed in an atomic calculation, it is expected to reveal that the internal motion of the electrons and the nucleus occurs around the center of mass. When the electrons are excited to higher electronic states the motion of the particles forming the atom becomes more complex. In this work we use plots of the electronic and nuclear densities to describe this motion. The densities are calculated with respect to the center of mass of the atom. In Rydberg states, which are subject of the present study, when one of the electrons moves away from the nucleus as it occupies states with a higher energy and with a larger average radius, the nucleus also starts to orbit around the center of mass with a larger radius. Also, in the process of Rydberg excitation, the electronic wave function acquires more radial nodes which the electronic density plot should reveal. Corresponding nodes should also appear in the nuclear density. A part of the present work is devoted to the analysis of the electronic and nuclear densities of the two major isotoplogues, ^{6}Li and ^{7}Li, of lithium.

As mentioned, the lowest eight ^2S Rydberg states of lithium were subject of previous high accuracy calculations (i.e. states $2s$, $3s$, …, $9s$). Apart from recalculating these eight states, in the calculations perform in this work, we also consider four more states (i.e. states $10s$, $11s$, $12s$, and $13s$) and transitions involving these states.

2. Method used in the calculations

The total non-relativistic Hamiltonian of an n-electron atom is first expressed in terms of laboratory Cartesian coordinates $\{\mathbf{R}_i\}$. The BO approximation is not assumed and, thus, the Hamiltonian describes a $(n+1)$-particle system consisting of a nucleus and n electrons. It depends on $3(n+1)$ coordinates, $\mathbf{R}_i$, $i = 1, ..., n+1$. Next separation of the motion of the center of mass [18] is performed. It effectively reduces the $(n+1)$-particle problem to an n-particle problem. To perform the separation a new Cartesian coordinate system is introduced whose first three coordinates are the laboratory coordinates of the center of mass, $\mathbf{R}_{CM}$, and the remaining $3n$ coordinates are internal coordinates. The internal coordinates are the position coordinates of the electrons relative to the position of the nucleus. The vector with length $3n$ of the internal coordinate is denoted by $\mathbf{r}$. It consists of single-electron position vectors $\mathbf{r}_i$, $i = 1, ..., n$. When the total Hamiltonian is transformed from the laboratory coordinate system to the new system of coordinates, it separates into the Hamiltonian representing the kinetic energy of the center-of-mass motion (dependent only on the center-of-mass coordinates) and the so-called internal Hamiltonian (dependent only on the internal coordinates). The separation is rigorous. The internal Hamiltonian, H_{nr}, has the following form (in a.u.):

$$\hat{\mathrm{H}}_{\mathrm{nr}} = -\frac{1}{2}\left(\sum_{i=1}^{n}\frac{1}{\mu_i}\nabla_{\mathbf{r}_i}^2 + \sum_{i=1}^{n}\sum_{j\neq i}^{n}\frac{1}{m_0}\nabla_{\mathbf{r}_i}^T\cdot\nabla_{\mathbf{r}_j}\right) + \sum_{i=1}^{n}\frac{q_0 q_i}{r_i} + \sum_{i=1}^{n}\sum_{j<i}^{n}\frac{q_i q_j}{r_{ij}}, \tag{1}$$

where q_0 is the nuclear charge, $q_i = -1$, $i = 1, ..., n$, are charges of the electrons, m_0 is the mass of the nucleus ($10961.89865 m_e$ for ^{6}Li and $12786.39228 m_e$ for ^{7}Li, where m_e is the electron mass), $m_i = m_e$, $i = 1, ..., n$ are the electron masses, and $\mu_i = m_0 m_i/(m_0 + m_i)$, $i = 1, ..., n$, are the reduced masses of the electrons. "T" denotes the transposition. The finite-nuclear-mass effects are represented by the mass-polarization term, $\sum_{i=1}^{n}\sum_{j\neq i}^{n}\frac{1}{m_0}\nabla_{\mathbf{r}_i}^T\cdot\nabla_{\mathbf{r}_j}$, and by the reduced masses, μ_i.

The standard procedure to account for the leading relativistic and QED effects is to expand the total energy in powers of the fine structure constant [20,21]:

$$E_{\mathrm{tot}} = E_{\mathrm{nr}}^{(0)} + \alpha^2 E_{\mathrm{rel}}^{(2)} + \alpha^3 E_{\mathrm{qed}}^{(3)} + \alpha^4 E_{\mathrm{qed}}^{(4)} + ..., \tag{2}$$

where $E_{\mathrm{nr}}^{(0)}$ is an eigenvalue of the nonrelativistic Hamiltonian (1), $E_{\mathrm{rel}}^{(2)}$

Table 1
$2s$, $3s$, …, and $10s\,^2S$ states of the lithium atom. The basis-set convergence of the total nonrelativistic energies, E_{nr}, the mass-velocity and orbit-orbite relativistic corrections, $\langle\hat{H}_{MV}\rangle$ and $\langle\hat{H}_{OO}\rangle$, the expectation values of the one-electron and two electron Dirac delta functions, $\langle\widetilde{\delta}(\mathbf{r}_i)\rangle$ and $\langle\widetilde{\delta}(\mathbf{r}_{ij})\rangle$, and the Araki-Sucher QED term, $\langle\mathscr{P}(1/r_{ij}^3)\rangle$. The convergence is only shown for the ^{7}Li isotopologue. The results for the ^{6}Li isotopologue and for $^\infty$Li are only shown for the largest basis sets (the $^\infty$Li results are obtained using a simple polynomial-based extrapolation procedure). All values are in atomic units.

State	Isotope	Basis Size	E_{nr}	$\langle\hat{H}_{MV}\rangle$	$\langle\delta^3(\mathbf{r}_i)\rangle$	$\langle\delta^3(\mathbf{r}_{ij})\rangle$	$\langle\hat{H}_{OO}\rangle$	$\langle\mathscr{P}(1/r_{ij}^3)\rangle$
2s	^{7}Li	8500	−7.477451930724	−78.53115335	4.61310856426	0.181401118401	−0.445491034	0.091267
	^{7}Li	9500	−7.477451930726	−78.53115335	4.61310856428	0.181401118406	−0.445491034	0.091268
	^{7}Li	10500	−7.477451930728	−78.53115342	4.61310856430	0.181401118409	−0.445491034	0.091267
	^{7}Li	∞	−7.477451930731(1)	−78.53115329(5)	4.61310856432(1)	0.181401118412(2)	−0.445491034(1)	0.091271(5)
	^{6}Li	10500	−7.477350681408	−78.52699808	4.61292633953	0.181394391273	−0.447137156	0.091300
	$^\infty$Li	10500	−7.478060323906	−78.55612563	4.61420361871	0.181441544285	−0.435597832	0.091068
3s	^{7}Li	9000	−7.353500488176	−77.8326780	4.57774746474	0.178682923795	−0.439699432	0.065939
	^{7}Li	10000	−7.353500488181	−77.8326785	4.57774746485	0.178682923806	−0.439699432	0.065936
	^{7}Li	11000	−7.353500488185	−77.8326786	4.57774746492	0.178682923812	−0.439699432	0.065936
	^{7}Li	∞	−7.353500488193(2)	−77.8326791(4)	4.57774746509(6)	0.178682923827(6)	−0.439699444(5)	0.065936(1)
	^{6}Li	11000	−7.353400979505	−77. 8285605	4.57756660642	0.178676287169	−0.441328521	0.065970
	$^\infty$Li	11000	−7.354098421437	−77.8574270	4.57883430865	0.178722805865	−0.429908606	0.065733
4s	^{7}Li	9500	−7.317935842537	−77.696396	4.5710163190	0.17817468483	−0.4384984	0.06159
	^{7}Li	10500	−7.317935842546	−77.696396	4.5710163191	0.17817468484	−0.4384984	0.06160
	^{7}Li	11500	−7.317935842552	−77.696393	4.5710163193	0.17817468487	−0.4384984	0.06168
	^{7}Li	∞	−7.317935842564(4)	−77.696391(4)	4.5710163199(4)	0.17817468495(5)	−0.4384983(2)	0.06184(7)
	^{6}Li	11500	−7.317836821409	−77.692282	4.5708357170	0.17816806483	−0.4401242	0.06172
	$^\infty$Li	11500	−7.318530845984	−77.721098	4.5721016234	0.17821446717	−0.4287278	0.06148
5s	^{7}Li	10000	−7.30295779418	−77.65284	4.5688887225	0.17801492772	−0.4381114	0.06014
	^{7}Li	11000	−7.30295779422	−77.65283	4.5688887226	0.17801492786	−0.4381114	0.06041
	^{7}Li	12000	−7.30295779423	−77.65283	4.5688887230	0.17801492791	−0.4381114	0.06050
	^{7}Li	∞	−7.30295779429(2)	−77.65281(1)	4.5688887236(4)	0.17801492804(7)	−0.4381102(5)	0.06057(7)
	^{6}Li	12000	−7.30285897585	−77.64872	4.5687082011	0.17800831304	−0.4397361	0.06053
	$^\infty$Li	12000	-7.30355157919	−77.67752	4.5699735440	0.17805467913	−0.4283472	0.06030
6s	^{7}Li	10500	−7.29526634660	−77.63485	4.568013398	0.1779493626	−0.4379510	0.05861
	^{7}Li	11000	−7.29526634664	−77.63485	4.568013399	0.1779493628	−0.4379510	0.05876
	^{7}Li	12500	−7.29526634670	−77.63485	4.568013401	0.1779493630	−0.4379510	0.05883
	^{7}Li	∞	−7.29526634680(8)	−77.63484(2)	4.568013403(2)	0.1779493638(9)	−0.4379506(5)	0.05886(1)
	^{6}Li	12500	−7.29516763164	−77.63074	4.567832912	0.1779427502	−0.4395752	0.05886
	$^\infty$Li	12500	-7.29585951074	−77.65953	4.569098024	0.1779891016	−0.4281895	0.05862
7s	^{7}Li	11000	−7.29079946806	−77.62623	4.567589139	0.177917617	−0.43787307	0.0553
	^{7}Li	12000	−7.29079946836	−77.62620	4.567589155	0.177917621	−0.43787304	0.0559
	^{7}Li	13000	−7.29079946853	−77.62612	4.567589158	0.177917626	−0.43787298	0.0574
	^{7}Li	∞	−7.29079946858(4)	−77.62594(10)	4.567589161(1)	0.177917635(5)	−0.43787291(4)	0.0592(6)
	^{6}Li	13000	−7.29070081316	−77.62202	4.567408685	0.177911015	−0.43949698	0.0574
	$^\infty$Li	13000	-7.29139227383	−77.65081	4.568673685	0.177957359	−0.42811278	0.0572
8s	^{7}Li	11500	−7.2879772464	−77.62149	4.56735880	0.177900396	−0.4378309	0.0537
	^{7}Li	12500	−7.2879772505	−77.62147	4.56735899	0.177900412	−0.4378308	0.0543
	^{7}Li	13500	−7.2879772518	−77.62145	4.56735905	0.177900420	−0.4378307	0.0550
	^{7}Li	∞	−7.2879772527(8)	−77.62138(9)	4.56735910(4)	0.177900426(3)	−0.4378305(4)	0.0557(3)
	^{6}Li	13500	−7.2878786340	−77.61735	4.56717859	0.177893809	−0.4394546	0.0550
	$^\infty$Li	13500	−7.2885698313	−77.64613	4.56844352	0.177940149	−0.4280712	0.0548
9s	^{7}Li	12000	−7.2860811502	−77.61882	4.56722344	0.177890259	−0.4378061	0.051
	^{7}Li	13000	−7.2860811531	−77.61863	4.56722358	0.177890299	−0.4378058	0.054
	^{7}Li	14000	−7.2860811547	−77.61858	4.56722364	0.177890310	−0.4378057	0.056
	^{7}Li	∞	−7.2860811556(7)	−77.61855(3)	4.56722368(2)	0.177890319(7)	−0.4378051(8)	0.058(7)
	^{6}Li	14000	−7.2859825621	−77.61448	4.56704318	0.177883700	−0.4394295	0.056
	$^\infty$Li	14000	−7.2866735829	−77.64326	4.56830808	0.177930037	−0.4280466	0.056
10s	^{7}Li	12500	−7.284746119	−77.61769	4.5671373	0.17788369	−0.4377923	0.041
	^{7}Li	13500	−7.284746140	−77.61759	4.5671381	0.17788374	−0.4377921	0.043
	^{7}Li	14500	−7.284746147	−77.61723	4.5671381	0.17788381	−0.4377914	0.047
	^{7}Li	∞	−7.284746150(25)	−77.61700(50)	4.5671380(3)	0.17788380(5)	−0.4377915(5)	0.048(5)
	^{6}Li	14500	−7.284647573	−77.61313	4.5669576	0.17787720	−0.4394152	0.047
	$^\infty$Li	14500	−7.285338469	−77.64191	4.5682225	0.17792354	−0.4280325	0.047

represents the leading relativistic corrections, $E_{qed}^{(3)}$ represents the leading QED corrections, and $E_{qed}^{(4)}$ represents higher-order QED corrections. α is the fine structure parameter; $\alpha = 7.2973525698\,10^{-3}$ [22]. In the tables, where the results of the present calculations are reported, term "rel" denotes $E_{rel}^{(2)}$, term "QED" denotes $E_{qed}^{(3)}$, and term "HQED" denotes $E_{qed}^{(4)}$.

As mentioned the $E_{rel}^{(2)}$ corrections are evaluated in this work in the framework of the perturbation theory using the non-BO non-relativistic wave function corresponding to zero-order energy $E_{nr}^{(0)}$. These corrections are expectation values of the respective effective Dirac–Breit

Table 2
11s, 12s, and 13s ^2S states of the lithium atom. The basis-set convergence of the total nonrelativistic energies, E_{nr}, the mass-velocity and orbit-orbite relativistic corrections, $\langle \hat{H}_{MV} \rangle$ and $\langle \hat{H}_{OO} \rangle$, the expectation values of the one-electron and two electron Dirac delta functions, $\langle \tilde{\delta}(\mathbf{r}_i) \rangle$ and $\langle \tilde{\delta}(\mathbf{r}_{ij}) \rangle$, and the Araki-Sucher QED term, $\langle \mathscr{P}(1/r_{ij}^3) \rangle$. The convergence is only shown for the ^{7}Li isotopologue. The results for the ^{6}Li isotopologue and for $^\infty$Li are only shown for the largest basis sets (the $^\infty$Li results are obtained using a simple polynomial-based extrapolation procedure). All values are in atomic units.

State	Isotope	Basis Size	E_{nr}	$\langle \hat{H}_{MV} \rangle$	$\langle \hat{H}_{OO} \rangle$	$\langle \delta^3(\mathbf{r}_i) \rangle$	$\langle \delta^3(\mathbf{r}_{ij}) \rangle$	$\langle \mathscr{P}(1/r_{ij}^3) \rangle$
11s	^{7}Li	14000	−7.28377022	−77.6172	4.567064	0.1778780	−0.437792	0.024
	^{7}Li	15000	−7.28377070	−77.6171	4.567071	0.1778786	−0.437789	0.028
	^{7}Li	16000	−7.28377074	−77.6168	4.567076	0.1778790	−0.437786	0.033
	^{7}Li	∞	−7.28377075(50)	−77.6170(2)	4.567075(5)	0.1778790(5)	−0.437785(5)	0.030(5)
	^{6}Li	16000	−7.28367218	−77.6127	4.566896	0.1778724	−0.439410	0.034
	$^\infty$Li	16000	−7.28436299	−77.6415	4.568160	0.1779187	−0.428027	0.033
12s	^{7}Li	14000	−7.28303614	−77.6153	4.567032	0.1778761	−0.437776	0.040
	^{7}Li	15000	−7.28303638	−77.6153	4.567035	0.1778764	−0.437775	0.042
	^{7}Li	16000	−7.28303645	−77.6154	4.567036	0.1778764	−0.437775	0.042
	^{7}Li	∞	−7.28303650(50)	−77.6155(2)	4.567040(5)	0.1778765(5)	−0.437775(5)	0.045(5)
	^{6}Li	16000	−7.28293790	−77.6113	4.566856	0.1779187	−0.439399	0.042
	$^\infty$Li	16000	−7.28362864	−77.6400	4.568121	0.1779162	−0.428016	0.042
13s	^{7}Li	14000	−7.28246797	−77.6155	4.566976	0.1778722	−0.437776	0.021
	^{7}Li	15000	−7.28246883	−77.6155	4.566987	0.1778727	−0.437778	0.024
	^{7}Li	16000	−7.28246913	−77.6156	4.566993	0.1778729	−0.437778	0.025
	^{7}Li	∞	−7.28246900(100)	−77.6155(2)	4.566995(10)	0.1778730(5)	−0.437780(5)	0.025(5)
	^{6}Li	16000	−7.28237059	−77.6115	4.566813	0.1778663	−0.439402	0.025
	$^\infty$Li	16000	−7.28306127	−77.6403	4.568078	0.1779126	−0.428018	0.025

Hamiltonians in the Pauli approximation [23,24] expressed in terms of the internal coordinates. For the ^2S Rydberg states of lithium considered in this work the relativistic Hamiltonian contains the following terms:

$$\hat{H}_{rel} = \hat{H}_{MV} + \hat{H}_{D} + \hat{H}_{OO} + \hat{H}_{SS}. \quad (3)$$

The terms represent the mass–velocity (MV), Darwin (D), orbit–orbit (OO), and spin–spin (SS) interactions (the spin-orbit interaction does not appear as it is zero for S states). The explicit form of the effective Dirac–Breit operators in the internal coordinates can be found in Ref. [18].

$E_{qed}^{(3)}$ according to the Eq. (11) in Ref. [8] that has the following form:

$$E_{qed}^{(3)} = \frac{4q_0}{3}\left[\frac{19}{30} + \ln(\alpha^{-2}) - \ln k_0\right]\sum_{i=1}^{n}\langle\delta^3(\mathbf{r}_i)\rangle + \left[\frac{164}{15} + \frac{14}{3}\ln\alpha\right]\sum_{i>j}\langle\delta^3(\mathbf{r}_{ij})\rangle - \frac{7}{6\pi}\sum_{i<j}\left\langle\mathscr{P}\left(\frac{1}{r_{ij}^3}\right)\right\rangle, \quad (4)$$

where $\ln k_0$ is the so-called Bethe logarithm [8] and $\left\langle\mathscr{P}\left(\frac{1}{r_{ij}^3}\right)\right\rangle$ is the Araki-Sucher term [8]. $\langle\delta^3(\mathbf{r}_i)\rangle$ and $\langle\delta^3(\mathbf{r}_{ij})\rangle$ are expectation values of the one-electron and two-electron three-dimensional Dirac delta functions. In our calculations, we do not include the term proportional to Bethe logarithm, $\ln k_0$.

The spatial parts of the wave functions of the twelve lowest ^2S states of lithium considered in this work are expanded in terms of following ECGs:

$$\phi_k = \exp[-\mathbf{r}^T\underline{\mathbf{A}}_k\mathbf{r}], \quad (5)$$

where $\underline{\mathbf{A}}_k$ is $3n \times 3n$ symmetric matrix. Basis functions (5) need to be square integrable in order to be used in expanding wave functions of bound states. This only happens if the $\underline{\mathbf{A}}_k$ matrix is positive definite. To make $\underline{\mathbf{A}}_k$ positive definite it is represented in the Cholesky-factored form as $\underline{\mathbf{A}}_k = (L_k L_k^T) \otimes I_3$, where L_k is a $n \times n$ lower triangular matrix, I_3 is a 3 unit matrix, and ⊗denotes the Kronecker product. With the L_k matrix elements being any real numbers, $\underline{\mathbf{A}}_k$ is positive definite. In the variational optimization performed in this work for the ECG basis set of each considered state the matrix elements of L_k are the variational parameters. Due to the above mentioned property of the Cholesky factorization they can be varied without any restrictions in the range form − ∞ to + ∞.

The spin-free formalism [25,26] is used to enforce the proper permutational symmetry of the wave function. In this formalism, a projector, which introduces the desired symmetry properties, is constructed using the standard procedure involving Young operators [27]. For the ^2S states of the lithium atom the symmetry projector can be chosen as: Y = (1 + P12)(1-P23), where Pij permutes the labels of the spatial coordinates of the i-th and j-th electrons. In the calculations of the Hamiltonian and overlap matrix elements, as well as in the operators representing the relativistic corrections, the projector Y is moved from the "bra" to the "ket" and appears as $P = Y^\dagger Y$ in the "ket" part of the integrals ($|\tilde{\phi}\rangle = P|\phi\rangle$).

In the approach used in this work the variational calculation for each state is performed separately and independently from other states. For each state a different basis set is generated by the minimization of the total energy of that state with respect to the L_k matrix elements. The linear expansion coefficients, c_k, of the wave function in terms of basis functions are obtained in the standard way by solving the secular equation.

The variational minimization of the second or a higher root of the nonrelativistic Hamiltonian requires the corresponding eigenfunction to be kept orthogonal to the eigenfunctions of the lower roots (MacDonald-Hylleraas-Undheim theorem). Even though the optimization of the ECG basis set and the generation of the wave function for each state is carried out in a separate calculation, the procedure used makes the calculated wave function orthogonal to the wave functions of all lower states expressed in terms of the basis set used in the calculation. Thus, all total energies obtained in this work are strict upper bounds to the corresponding exact energy values. However, the final wave functions obtained for different states are not, strictly speaking, exactly orthogonal to each other, as they are obtained in different basis sets. They would be exactly orthogonal if the basis sets are complete. As the total energies of the twelve considered states are uniformly very well converged, the deviation from the exact orthogonality of the final wave functions should be very small.

Growing the basis set is a multistep process. It involves choosing a small starting set of ECGs (for the lowest state this set is generated using an orbital guess obtained using a standard AO basis set; for a higher

Table 3
Computed $ns \rightarrow 2s$, $n = 2, ...,9$, transition frequencies (in cm^{-1}) for the lithium atom in comparison with the previously calculate values (Theo) and experimental results (Exp). The subscripts (nr, rel, rel + QED, and rel + HQED) indicate the inclusion of relativistic and QED corrections in the calculations. Tthe ∞Li results are obtained using a simple polynomial-based extrapolation procedure.

Transition	Isotope	Basis Size	ΔE_{nr}	ΔE_{rel}	$\Delta E_{rel+QED}$	$\Delta E_{rel+QED+HQED}$
$3s \rightarrow 2s$	^{7}Li	9000	27204.1971611	27206.286186	27205.917911	27205.912196
	^{7}Li	10000	27204.1971604	27206.286179	27205.917904	27205.912189
	^{7}Li	11000	27204.1971600	27206.286178	27205.917904	27205.912188
	^{7}Li	∞	27204.1971590(5)	27206.286170(5)	27205.917896(5)	27205.912181(5)
	^{7}Li	Theo [7]				27206.0937(6)
	^{7}Li	Exp [28]				27206.094072(3)
	^{6}Li	11000	27203.8151337	27205.904152	27205.535891	27205.530176
	^{6}Li	Theo [7]				27205.7166(6)
	^{6}Li	Exp [28]				27205.712008(6)
$4s \rightarrow 2s$	^{7}Li	9500	35009.7346525	35012.26234	35011.82389	35011.81709
	^{7}Li	10500	35009.7346510	35012.26235	35011.82390	35011.81709
	^{7}Li	11500	35009.7346500	35012.26238	35011.82392	35011.81711
	^{7}Li	∞	35009.7346480(8)	35012.26240(5)	35011.82392(5)	35011.81712(5)
	^{7}Li	Theo [8]				35012.0336(8)
	^{7}Li	Exp [29]				35012.03358(3)
	^{6}Li	11500	35009.2456218	35011.77335	35011.33490	35011.32810
	^{6}Li	Theo [8]				35011.5445(8)
	^{6}Li	Exp [29]				35011.54450(3)
$5s \rightarrow 2s$	^{7}Li	10000	38297.036292	38299.70838	38299.24776	38299.24061
	^{7}Li	11000	38297.036287	38299.70850	38299.24785	38299.24070
	^{7}Li	12000	38297.036283	38299.70854	38299.24787	38299.24073
	^{7}Li	∞	38297.036272(4)	38299.70871(15)	38299.24804(15)	38299.24090(15)
	^{7}Li	Theo [8]				38299.4688(8)
	^{7}Li	Exp [30]				38299.4627(10)
	^{6}Li	12000	38296.502755	38299.17498	38298.71434	38298.70719
	^{6}Li	Theo [8]				38298.9353(8)
	^{6}Li	Exp [30]				38298.9283(10)
$6s \rightarrow 2s$	^{7}Li	10500	39985.113916	39987.8463	39987.3766	39987.3693
	^{7}Li	11500	39985.113903	39987.8464	39987.3767	39987.3694
	^{7}Li	12500	39985.113895	39987.8464	39987.3767	39987.3694
	^{7}Li	∞	39985.113874(17)	39987.8464(2)	39987.3768(2)	39987.3695(2)
	^{7}Li	Theo [8]				39987.6015(8)
	^{7}Li	Exp [30]				39987.586(3)
	^{6}Li	12500	39984.557690	39987.2902	39986.8205	39986.8132
	^{6}Li	Theo [8]				39987.0452(8)
	^{6}Li	Exp [30]				39987.027(4)
$7s \rightarrow 2s$	^{7}Li	11000	40965.480437	40968.2409	40967.7671	40967.7598
	^{7}Li	12000	40965.480373	40968.2412	40967.7674	40967.7600
	^{7}Li	13000	40965.480335	40968.2421	40967.7681	40967.7607
	^{7}Li	∞	40965.480325(8)	40968.2442(13)	40967.7698(16)	40967.7624(16)
	^{7}Li	Theo [8]				40967.9944(8)
	^{6}Li	13000	40964.911029	40967.6726	40967.1986	40967.1913
	^{6}Li	Theo [8]				40967.4250(8)
$8s \rightarrow 2s$	^{7}Li	11500	41584.88651	41587.6630	41587.1869	41587.1795
	^{7}Li	12500	41584.88561	41587.6623	41587.1861	41587.1787
	^{7}Li	13500	41584.88531	41587.6622	41587.1860	41587.1786
	^{7}Li	∞	41584.88511(17)	41587.6629(10)	41587.1866(11)	41587.1792(11)
	^{7}Li	Theo [8]				41587.4098(8)
	^{6}Li	13500	41584.30776	41587.0847	41586.6086	41586.6012
	^{6}Li	Theo [8]				41586.8322(8)
$9s \rightarrow 2s$	^{7}Li	12000	42001.03151	42003.8159	42003.3386	42003.3312
	^{7}Li	13000	42001.03088	42003.8176	42003.3400	42003.3326
	^{7}Li	14000	42001.03053	42003.8178	42003.3401	42003.3327
	^{7}Li	∞	42001.03034(15)	42003.8180(4)	42003.3401(11)	42003.3327(11)
	^{7}Li	Theo [8]				42003.5462(8)
	^{6}Li	14000	42000.44745	42003.2349	42002.7572	42002.7498
	^{6}Li	Theo [8]				42002.9631(8)

state a basis set generated for the next lower state is used as the initial guess). Next small groups of functions are added to the basis set and, after each group is optimized, the whole basis set is reoptimized. The reoptimization involves cycling over all functions, one by one, several times and reoptimizing their nonlinear parameters. All optimizations are carried out using this one-function-at-the time approach. The initial guess for an added function is generated by selecting a set of most contributing functions already included in the basis set, randomly perturbing their non-linear parameters, and choosing the functions which lower the energy the most. The use of the analytic gradient is crucial in making the optimization efficient.

The above described strategy is found efficient and numerically

Table 4
Computed $ns \rightarrow 2s$, $n = 10, ...,13$, transition frequencies (in cm^{-1}) for the lithium atomi. The subscripts (nr, rel, rel + QED, and rel + HQED) indicate the inclusion of relativistic and QED corrections in the calculations. The $^{\infty}$Li results are obtained using a simple polynomial-based extrapolation procedure.

Transition	Isotope	Basis Size	ΔE_{nr}	ΔE_{rel}	$\Delta E_{rel+QED}$	$\Delta E_{rel+QED+HQED}$
$10s \rightarrow 2s$	^{7}Li	12500	42294.364	42297.147	42296.119	42296.111
	^{7}Li	13500	42294.360	42297.144	42296.115	42296.108
	^{7}Li	14500	42294.358	42297.146	42296.117	42296.109
	^{7}Li	∞	42294.357(5)	42297.148(8)	42296.119(8)	42296.111(8)
	^{6}Li	14500	42293.771	42296.559	42295.530	42295.522
$11s \rightarrow 2s$	^{7}Li	14000	42508.55	42511.33	42510.30	42510.29
	^{7}Li	15000	42508.45	42511.22	42510.20	42510.19
	^{7}Li	16000	42508.44	42511.22	42510.19	42510.18
	^{7}Li	∞	42508.43(10)	42511.21(11)	42510.19(11)	42510.18(11)
	^{6}Li	16000	42507.85	42510.63	42509.60	42509.59
$12s \rightarrow 2s$	^{7}Li	14000	42669.66	42672.46	42671.43	42671.42
	^{7}Li	15000	42669.61	42672.40	42671.37	42671.37
	^{7}Li	16000	42669.60	42672.39	42671.36	42671.35
	^{7}Li	∞	42669.59(10)	42672.38(11)	42671.35(11)	42671.34(11)
	^{6}Li	16000	42669.00	42671.80	42670.77	42670.76
$13s \rightarrow 2s$	^{7}Li	14000	42794.36	42797.14	42796.12	42796.11
	^{7}Li	15000	42794.18	42796.96	42795.93	42795.92
	^{7}Li	16000	42794.11	42796.89	42795.86	42795.86
	^{7}Li	∞	42794.14(20)	42796.92(22)	42795.89(22)	42795.89(22)
	^{6}Li	16000	42793.52	42796.30	42795.27	42795.26

stable. It allows at all stages of the basis growing and optimizing process to control and, if necessary, eliminate any linear dependency that may occur between the basis functions. As such dependencies may lead to numerical inaccuracies and may destabilize the calculation, they have to be eliminated.

In this work the variational optimization of the non-linear parameters of the Gaussians is carried out using the FNM approach and performed only for the ^{7}Li isotopologue. The ^{7}Li basis sets for all considered states are used in the calculations for the ^{6}Li isotopologue, as well as the INM energy calculations (for $^{\infty}$Li) without reoptimization of the ECG non-linear parameters. As our previous calculations of atomic isotopologues have shown [19], no reoptimization of the nonlinear variational parameters is needed when states of different isotopes are calculated. The adjustment of the linear coefficients, c_k, through rediagonalization of the Hamiltonian matrix suffices to describe relatively small changes in the wave function and the energy caused by a change of the nuclear mass.

As mentioned in the introduction, the FNM approach used in the present calculations allows to describe the coupled motion of both electrons and the nuclei using nuclear and electron density plots. The electron density, ρ_e at point $\boldsymbol{\xi}$ relative to the center of mass of the atom, $\mathbf{R}_{CM}$, is evaluated as the expectation value of the following 3D Dirac delta function:

$$\rho_e(\boldsymbol{\xi}) = < \delta(\mathbf{R}_e - \mathbf{R}_{CM} - \boldsymbol{\xi}) > , \quad (6)$$

where $\mathbf{R}_e$ is the position vector of one of the electrons in the laboratory coordinate system. As the FNM ECG wave function is used in the expectation value calculation, slightly different densities are obtained for ^{6}Li and ^{7}Li. The nuclear density, ρ_n, at point $\boldsymbol{\xi}$, is evaluated in a similar way as the expectation value of the following delta function:

$$\rho_n(\boldsymbol{\xi}) = < \delta(\mathbf{R}_n - \mathbf{R}_{CM} - \boldsymbol{\xi}) > , \quad (7)$$

where $\mathbf{R}_n$ is the position vector of nucleus in the laboratory coordinate system. Electronic and nuclear density plots for some selected states of ^{6}Li and ^{7}Li are compared in the result section.

3. Results

The ECG atomic code for S states written in Fortran90 and employing the MPI (message passing interface) is used in the present calculations. The considered twelve Rydberg ^{2}S states of lithium are divided into two groups. The first group comprising eight lowest states, $2s$, $3s$, …, and $9s$ was calculated with high accuracy before [8]. The second group comprising states $10s$, $11s$, $12s$, and $13s$ has not been calculated yet by others. The purpose of the calculations performed for the first group of states is to determine the accuracy of the calculations using ECGs with more accurate calculations performed with products of Slater-type orbitals multiplied by powers of the distances between the three electrons and the nucleus, r_1, r_2, and r_3, and by powers of inter-electron distances, r_{12}, r_{13}, and r_{23}. The results for states $2s$-$10s$ are collected in Table 1. The results for states $11s$-$13s$ are shown in Table 2. Both sets of results include the non-relativistic energies, E_{nr}, the mass-velocity and orbit-orbit relativistic corrections, $\langle \hat{H}_{MV} \rangle$ and $\langle \hat{H}_{OO} \rangle$, the expectation values of the one-electron and two electron Dirac delta functions, $\langle \delta^3(\mathbf{r}_i) \rangle$ and $\langle \delta^3(\mathbf{r}_{ij}) \rangle$, and the Araki-Sucher QED term, $\langle \mathscr{P}(1/r_{ij}^3) \rangle$. The convergence is only shown for the ^{7}Li isotopologue. The results for the ^{6}Li isotopologue and for $^{\infty}$Li are only given for the best basis sets. The $^{\infty}$Li results are obtained by setting the mass of the nucleus to infinity in the calculations (in practice, setting it to a large number).

The number of the basis functions used in the calculations varies from state to state. It increases with the excitation level of the atom. This is necessary because, as the excitation level increases, the wave functions become more oscillatory and this requires more basis functions to be used in the wave-function expansion. For the ground $2s$ state, the largest number of the ECGs used is 10500 and the results obtained with 8500, 9500, and 10,500 ECGs are shown in Table 1. For state $9s$ we show the results obtained with 12,000, 13,000, and 14,000 ECGs. For state $10s$ the largest basis set used comprises 14500 ECGs and for states $10s$, $11s$, $12s$, and $13s$ the largest set consists of 16000 ECGs. To assess the quality of the present results, one can compare, for example, the $^{\infty}$Li non-relativistic energies for the lowest two states with the recent values of Wang et al. [7] obtained with Hylleraas-type functions. Their energies of −7.478060323910150(5) and −7.354098421444367(3) hartree are lower than our energies obtained with ECGs in the 13-th decimal digit by 6 and 7, respectively.

The data from Table 1 and Table 2 are used to calculate the $ns \rightarrow 2s$ deexcitation transition frequencies for all twelve states considered in this work. The calculations are performed for both ^{6}Li and ^{7}Li isotopologues. The results are shown in Table 3 and Table 4. The results

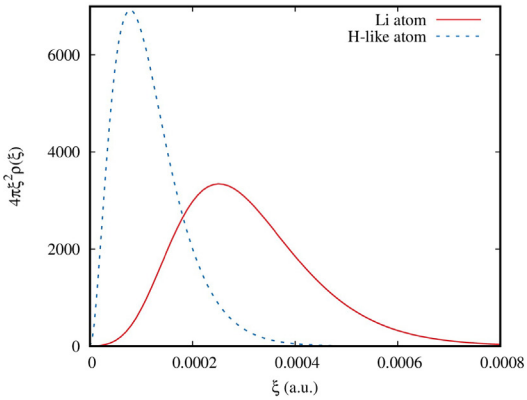

(a) state 2*s*.

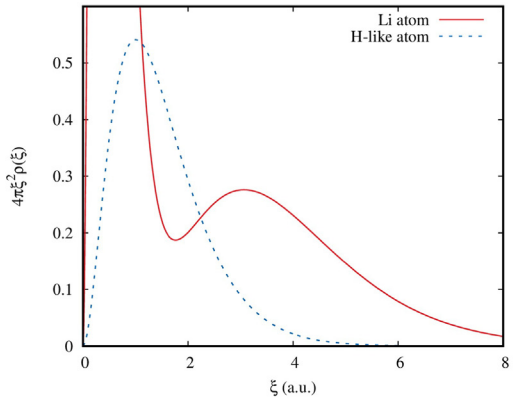

(b) state 2*s*.

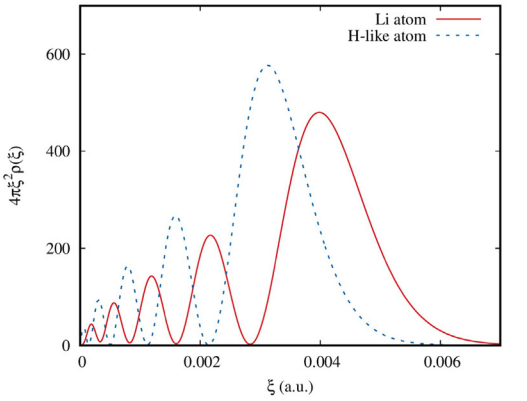

(c) state 6*s*.

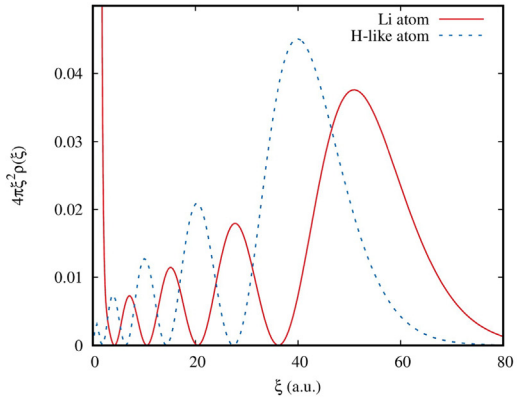

(d) state 6*s*.

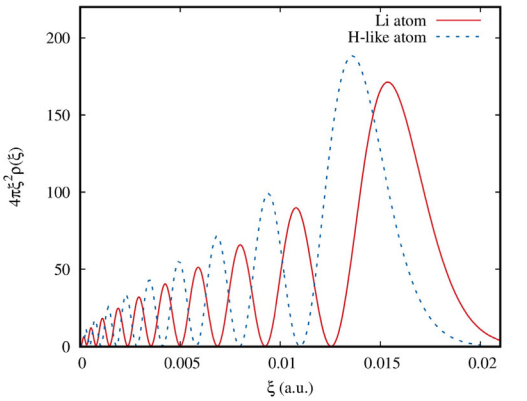

(e) state 11*s*.

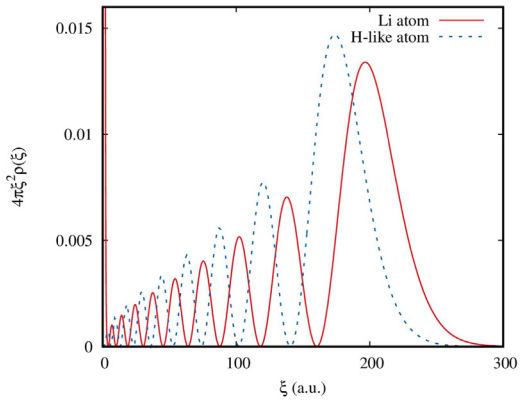

(f) state 11*s*.

Fig. 1. Radial nuclear densities of Rydberg states 2*s*, 6*s*, and 11*s* of ^{7}Li (plots a, c, and e), and the corresponding radial electron densities (plots b, d, and f. Both sets of densities shown with solid lines. Dash lines show densities of a hydrogen-like atom whose nuclear mass is equal to the nuclear mass of ^{7}Li and the nuclear charge is +1. The hydroge-like densities are included to show the Rydberg character of the ^{7}Li densities. The densities are calculated using Eqs. (7) and (6). They are multiplied by $4\pi r^2$ to make them be radial densities, as the considered states are spherically symmetric.

are compared with the previous calculations [2,7,8] and with experimental results [28–30].

In general, our results agree well with the results of the previous calculations [8]. The agreement is slightly worse for lower states than for the higher states. We attribute this to not including in the present calculations some higher order effects, which the previous calculations accounted for. The novelty of the present work are the predictions of the transition frequencies involving states 10*s*, 11*s*, 12*s*, and 13*s*. We estimate the reliability of these predictions to be by about one order of magnitude lower than for states 8*s*, 9*s*, and 10*s*.

As predicted by Lorenzen and Niemax [31], the value of the quantum defect effect should be approximately constant for a series of excitations of a valence electron to Rydberg states with a particular angular momentum quantum number. For the states considered in this work, the *ns* states, quantum defect effect is indeed almost constant and ranges from 0.41146 for the 2*s* state to 0.39831 for the 13*s* state. The quantum defect effect for the ^2S Rydberg series was analyzed by Bubin and Adamowicz [32] and two models were tested for more accurate prediction of the transition energies of the states in the series with respect to the ground $^2S1s^2$ 2*s* state using QDE-like formulas fitted to the experimental transitions. For states 10*s*, 11*s*, 12*s*, and 13*S*, the more sophisticated of the two models (Model 2) predicted the transition

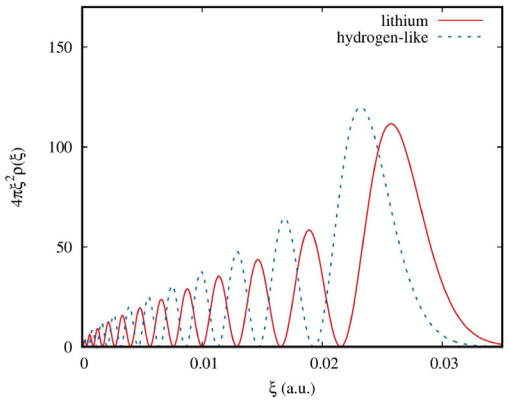

(a) state 13s of ^{6}Li.

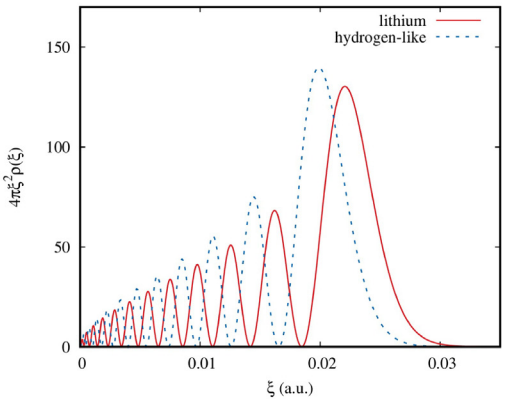

(b) state 13s of ^{7}Li.

Fig. 2. Radial nuclear densities of Rydberg state 13s of ^{6}Li (plot a) and ^{7}Li (plot b). Dash lines show densities of a hydrogen-like atom whose nuclear mass is equal to the nuclear mass of ^{6}Li in (a) and to the nuclear mass of ^{7}Li in (b) and the nuclear charge is +1. The hydroge-like densities are included to show the Rydberg character of the ^{7}Li densities. The densities are calculated using Eqs. (7) and (6). They are multiplied by $4\pi r^2$ to make them be radial densities, as the considered states are spherically symmetric.

energies to be 42295.82, 42509.73, 42670.72, and 42794.93 cm^{-1}, respectively, for ^{6}Li, and 42296.41, 42510.32, 42671.32, and 42795.52 cm^{-1}, respectively, for ^{7}Li. These values are in good agreements with the transition frequencies calculated in the present work of 42295.522, 42509.59, 42670.76, and 42795.26 cm^{-1} for ^{6}Li, and 42296.109, 42510.18, 42671.35, and 42795.85 cm^{-1} for ^{7}Li.

The $ns \rightarrow 2s$ deexcitation transition frequencies calculated for ^{7}Li and ^{6}Li enable calculation of the isotope shifts of the corresponding transitions. As these shifts can be measured experimentally, their theoretical prediction may provide valuable information for such measurements. In moving from the ^{7}Li to ^{6}Li transitions, a down-shift of the transitions is predicted. The shift is equal to $-0.38\,cm^{-1}$ for the $3s \rightarrow 2s$ transition, to $-0.49\,cm^{-1}$ for the $4s \rightarrow 2s$, and to -0.53, -0.56, -0.57, -0.58, -0.58, -0.59, -0.59, -0.58, and $-0.60\,cm^{-1}$ for the $ns \rightarrow 2s$, $n = 5, ...,13$, transitions, respectively.

To illustrate the nature of the twelve ^2S Rydberg states calculated in this work with the FNM approach we show plots of the nuclear and electronic densities for some selected states (states 2s, 6s, and 11s). The density plots are shown in Fig. 1. The densities are calculated with the approach described in the methodology section. As mentioned, the plots provide a representation of the coupled motion of the electrons and the nucleus around the center of mass of the atom. This should be manifested by the number and the character of the maxima of the electron densities matching the maxima in the nuclear densities. Naturally, as the mass of the nucleus is much larger than the electronic mass, the radius of the motion of the nucleus around the center of mass and, consequently, the distances of the maxima from the center of mass in the nuclear density should be much smaller than those in the electronic density (the distance of the maxima in the two densities should scale as the ratio of the nuclear and electronic masses). Upon analysis of the plots, this is indeed what one observes. It is also interesting to compare the densities obtained for the ^{6}Li and ^{7}Li isotopologues. One may expect that the electronic densities of the two isotopologues for a particular state should be almost identical. However, the peaks in the nuclear densities of ^{7}Li should be shifted closer by about 20% to the center of mass in comparison to the peaks in the ^{6}Li density (the masses of the two isotopologues differ by about 20%). Indeed, one can notice such as a shift in the nuclear-density plots for state 13s shown in Fig. 2. Also, as one can notice, as the electronic density becomes increasingly more diffuse with the increasing level of the excitation, the nuclear density also diffuses in space. This is a reflection of the average distances of both the electrons and the nucleus from the center of mass of the atom increasing with the excitation level.

4. Summary

In summary, explicitly correlate all-electron Gaussian functions are used to calculate the lowest twelve ^2S Rydberg states of the lithium atom. While for states 2s, 3s, ..., and 9s high-accuracy calculations have been done before [8], the calculations of states 10s, 11s, 12s, and 13s presented in this work are done for the first time. The total energies of the twelve states include the leading relativistic and QED corrections. These energies are used to calculate transition frequencies corresponding to de-exciting the atom from each of the states to the 2s ground state. These frequencies are compared with the results of the previous calculations [8] and with the high-resolution experimental results [28–30]. The comparison shows that the present results are consistent with the previous results. This lends credence to the predicted transitions involving states 10s, 11s, 12s, and 13s. These predictions can be used to experimentally measure these frequencies. As the method employed in the present calculations uses the finite-nuclear-mass approach, slightly different sets of transitions are obtained for ^{6}Li and ^{7}Li. The isotope shifts, which can be derived from the present results, are also measurable quantities that can be determined experimentally.

The finite-nuclear-mass approach used in the present work enables an analysis of the coupling to the motions of the electrons and the nucleus around the center of mass of the atom. In this work the analysis is performed using the electronic and nuclear densities. These densities are determined relative to the center of mass of the atom and plotted as functions of the distance from this center. As expected, as the level of the Rydberg excitation increases the electronic density becomes increasingly more oscillatory and diffuse. Due to the coupling of the electronic and nuclear motions similar oscillations appear in the nuclear density. For each maximum in the electronic density there is a matching maximum in the nuclear density. The relative heights of the maxima in the electronic density are similar to the maxima heights in the nuclear density. However, the two densities differ in terms of their radial extent, with the extent of the nuclear density being much more compressed towards the center of mass than the electronic density. The compression ratio is equal to the electron/nucleus mass ratio.

Declaration of Competing Interest

The authors declared that there is no conflict of interest.

Acknowledgments

A.B. acknowledges support from the Shakhmardan Yessenov Foundation. S.B. acknowledges funding from MESRK state-targeted program BR05236454 and NU faculty development grant 090118FD5345. The work of M.S has been supported by the Polish National Science Centre, grant DEC-2013/10/E/ST4/00033. The authors are grateful to Prof. Gordon W. F. Drake (University of Windsor) for useful discussions. The authors are also grateful to the University of Arizona Research Computing and Nazarbayev University Library and IT Services for providing computational resources for this work.

References

[1] K. Ishida, H. Nakatsuji, Chem. Phys. Lett. 19 (1973) 268.
[2] G.W.F. Drake, Zong-Chao Yan, Phys. Rev. A 46 (1992) 2378.
[3] J.S. Sims, S.A. Hagstrom, Phys. Rev. A 80 (2009) 052507.
[4] F.W. King, Int. J. Quantum Chem. 113 (2013) 2534.
[5] M.B. Ruiz, J.T. Margraf, A.M. Frolov, Phys. Rev. 88 (2013) 012505.
[6] C.H. Leong, I. Porras, F.W. King, J. Math. Chem. 54 (2016) 1514.
[7] L.M. Wang, C. Li, Z.-C. Yan, G.W.F. Drake, Phys. Rev. A 95 (2017) 032504.
[8] M. Puchalski, D. Ke˛dziera, K. Pachucki, Phys. Rev. 82 (2010) 062509.
[9] M. Stanke, J. Komasa, S. Bubin, L. Adamowicz, Phys. Rev. A 80 (2009) 022514.
[10] M. Puchalski, K. Pachucki, J. Komasa, Phys. Rev. A 89 (2014) 012506.
[11] S. Bubin, L. Adamowicz, Phys. Rev. Lett. 118 (2017) 043001.
[12] S.F. Boys, Proc. R. Soc. London, A 258 (1960) 402.
[13] M. Stanke, D. Ke˛dziera, S. Bubin, L. Adamowicz, Phys. Rev. Lett. 99 (2007) 043001.
[14] L. Johansson, Ark. Fys. 23 (1963) 119.
[15] A. Kramida, W.C. Martin, J. Phys. Chem. Ref. Data 26 (1997) 1185.
[16] D.B. Kinghorn, L. Adamowicz, Phys. Rev. Lett. 83 (1999) 2541.
[17] P.M. Kozlowski, L. Adamowicz, J. Chem. Phys. 96 (1992) 9013.
[18] S. Bubin, M. Pavanello, W.-Ch. Tung, K.L. Sharkey, L. Adamowicz, Chem. Rev. 113 (2013) 36.
[19] J. Mitroy, S. Bubin, W. Horiuchi, Y. Suzuki, L. Adamowicz, W. Cencek, K. Szalewicz, J. Komasa, D. Blume, K. Varga, Rev. Mod. Phys. 85 (2013) 693.
[20] W.E. Caswell, G.P. Lepage, Phys. Lett. B 167 (1986) 437.
[21] K. Pachucki, Phys. Rev. A 56 (1997) 297.
[22] P.J. Mohr, B.N. Taylor, D.B. Newell Rev, Mod. Phys. 84 (2012) 1527.
[23] H.A. Bethe, E.E. Salpeter, Quantum Mechanics of One- and Two-Electron Atoms, Plenum, New York, 1977.
[24] A.I. Akhiezer, V.B. Berestetskii, Quantum Electrodynamics, John Wiley & Sons, New York, 1965.
[25] F.A. Matsen, R. Pauncz, The Unitary Group in Quantum Chemistry, Elsevier, Amsterdam, 1986.
[26] R. Pauncz, Spin Eigenfunctions, Plenum, New York, 1979.
[27] M. Hamermesh, Group Theory and Its Application to Physical Problems, Addison-Wesley, Reading, MA, 1962.
[28] Y.-H. Lien, K.-J. Lo, H.-C. Chen, J.-R. Chen, J.-Y. Tian, J.-T. Shy, Y.-W. Liu, Phys. Rev. A 84 (2011) 042511.
[29] W. DeGraffenreid, C.J. Sansonetti, Phys. Rev. A 67 (2003) 012509.
[30] L.J. Radziemski, R. Engleman, J.W. Brault, Phys. Rev. A 52 (1995) 4462.
[31] C.J. Lorenzen, K. Niemax, Phys. Scripta 27 (1983) 300.
[32] S. Bubin, L. Adamowicz, Phys. Rev. A 87 (2013) 042510.